Journal of Thermal Analysis and Calorimetry, Vol. 79 (2005) 33–38

BIODEGRADABLE POLYMERS
Part II. Thermal degradation of biodegradable plastics cross-linked from formaldehyde-soy protein concentrate

S. N. Swain[1], *K. K. Rao*[2] *and P. L. Nayak*[1]*

[1]Biodegradable Polymer Research Laboratory, Department of Chemistry, Ravenshaw College, Cuttack 753 003, India
[2]Regional Research Laboratory [CSIR], Bhubaneswar, India

Soy protein concentrate, a biodegradable renewable resource agricultural biopolymer, has been cross-linked with formaldehyde for better processing material. Thermogravimetric analysis of the biopolymer has been followed using a computer analysis method, Lotus package, developed by us for assigning the degradation mechanism. A number of equations have been used to evaluate the kinetic parameters. The mechanism of degradation of the biopolymer is explained on the basis of the kinetic parameters.

Keywords: *cross-linked, degradation, formaldehyde, soy-protein*

Introduction

The environmental impact of persistent plastic wastes from disposable materials is growing more acute world wide. Approximately 1 million metric tons of plastics waste were discarded in 1992, and this figure is expected to reach 1.54 million metric tons by 2004 [1]. Alternate disposal methods are insufficient. Incineration can generate toxic air pollution, and satisfactory landfill sites are limited. Since petroleum resources are finite and are becoming limited, the cost of petroleum-based plastics is steadily increasing, and most countries must import these resources. Hence, there is a need to focus attention on renewable resources for manufacturing biodegradable plastic raw materials [2, 3].

Abundant plant-based proteins are available from renewable resources and agriculture processing by-products, such as soybean proteins from oil processing and gluten proteins from corn or wheat-starch production. For example, soybean contains about 40% protein, and the United States produces about 52% of the total world soybean crops. Utilizing these protein by-products for the manufacture of biodegradable resins will help alleviate the environmental problems and add value to agricultural by-products [1].

Soy proteins have commonly been used for food and animal feed for many years. However, soy protein is a new biopolymer for biodegradable resins. Soy protein polymers are macromolecules that contain a number of amino acids at the side chains. Major protein components include 2S, 7S, 11S and 15S fractions, classified by their ultra-centrifugal sedimentation rates.

The 7S fraction makes up approximately one third of the total soybean proteins, and its main component is 7S globulin. The 11S fraction is roughly 50% of soybean proteins, and contains a single component called 11S globulin [4]. Physiochemical properties of 7S and 11S globulin have been extensively studied in food applications [5–11].

Soy protein possesses many side reactive groups such as $–NH_2$, –OH and –SH which are susceptible to cross-linking reactions, in addition to naturally existing disulfide cross-links. Cross-linking leads to the formation of larger aggregates accompanied by an increase in molecular mass, reduction of solubility and reduced elasticity [12]. Investigations by several authors have shown that unmodified soy proteins were highly hydrophilic and plastics made from them are water sensitive resulting in poor mechanical properties [13, 14]. Aldehydes such as formaldehyde, furfuraldehyde and glyoxal could be used as cross-linkers to modify the properties of soy protein for better processable material and industrial applications.

In the present research programme, formaldehyde has been used as a cross-linking agent to modify soy-protein concentrate for better commercial value. The degradation behaviour of the cross-linked soy-protein concentrate has been monitored by TG analysis. A novel LOTUS package computerized method developed by us has been used for evaluating the kinetic parameters using several kinetic equations. The values of the energy of activation have been determined using this method and the degradation steps have been explained on the basis of these parameters.

* Author for correspondence: nayakpl@sify.com

1388–6150/$20.00

Akadémiai Kiadó, Budapest, Hungary
Springer, Dordrecht, The Netherlands

Experimental

Materials

Soy protein concentrate with protein content about 70% was obtained from Archor Daniels, Midland [Decatur, IL, USA] as gift sample, and was used for the reaction. Formaldehyde [GR] obtained from Germany [Merck], was used for cross-linking reaction.

Preparation of cross linked soy protein concentrate

Soy protein concentrate was mixed with distilled water at a ratio of 1:10. The slurry was continuously stirred with a mechanical stirrer and then formaldehyde was added drop wise (0.5, 1, 2.5, 5 and 7.5 mass/mass%) dry base of soy concentrate]. The mixture was allowed to stand for 18 to 24 h. The pH was then adjusted to 4.5 by adding acetic, propionic, citric and adipic acid, while the mixture was continuously stirred. The slurry was centrifuged to remove excess water (Sorvall Superspeed RC2-B; 4541 g, 10 min) and the precipitated residue was dried 24 h in a convection oven at 50°C. The dried modified soy concentrate (SC) was then milled (Cyclone Sample Mill, UDY Corporation, Fort Collins, CO) to pass through a 35 mesh sieve.

Thermogravimetric analysis

Thermal degradation pattern of the biopolymers were studied using thermogravimetric analyzer (TGA7, Perkin Elmer, Norwalk, CT) in air and scan temperature range was from room temperature to 800°C at 3°C min^{-1} increment. The thermal degradation data of the cross-linked soy-protein are furnished in Table 1.

Results and discussion

The foundation for the calculation of kinetic data from a TG curve is based on the formal kinetic Eq. (1).

$$-\frac{dx}{dt} = kx^n \quad (1)$$

where x is the amount of sample undergoing reaction, n is the order of reaction and k is the specific rate constant. The temperature dependence of k is expressed by the Arrhenius equation

$$k = Ae^{-E/RT} \quad (2)$$

where A is the pre-exponential factor, E is the activation energy and R is the universal gas constant. As discussed by Šesták [15], the relationship x to mass loss w, is represented by the following equation.

$$-dx = \frac{m_0}{W_\infty} dW \quad (3)$$

where m_0 is the initial mass of the sample and W_∞ is the maximum loss. By integration of the left hand side of Eq. (3) from m_0 to x and by integration of the right hand side from zero to W, the following equation is obtained.

$$X = \frac{m_0}{W_\infty}(W_\infty - W) \quad (4)$$

By substituting Eqs (2) and (4) into Eq. (1) and by differentiating the logarithmic form, an expression is obtained. This differential method is used by Freeman and Carroll [16].

Integral methods use the integrated form of Eq. (1) after the substitution of Eqs (3) and (4).

$$\left[\frac{m_0}{W_\infty}\right]^{1-n} = \int_0^W (W_\infty - W)^{-n} dW = A / \beta \int_{T_i}^{T_2} e^{-E/RT} dt \quad (5)$$

where β rate of heating and E, R, T have the usual meaning. The right hand side of the above equation can be solved by various methods and the final solution to the equation is an infinite series of which the first two terms are of interest. The methods are used by Doyle [17] and Coats and Redfern [18].

In the approximate methods, the right side of equation [5] is solved by an approximation using the temperature, T_i corresponding to the maximum rate of decomposition. This method is used by Horowitz and Metzger [19].

Of these three mathematical approaches, the integral method proposed by Coats and Redfern is exten-

Table 1 Thermal decomposition data of cross-linked SPC with 5% formaldehyde

Sample	Medium	Mass loss/% at various temperatures						
		100°C	200°C	300°C	400°C	500°C	600°C	700°C
SN6	propionic acid	2	3	23	51	61	73	90
SN9	citric acid	2	4	23	52	61	72	85
SN10	acetic acid	2	4	23	52	61	74	90
SN11	adipic acid	4	8	26	55	64	76	90

sively used in the estimation of kinetic parameters of thermal reactions. The final form of Coats and Redfern equation is

$$\ln\left[\frac{g(\alpha)}{T^2}\right] = \ln\left(\frac{AR}{\beta E}\right)\left[1-\left(\frac{2RT}{E}\right)\right] - E/RT \quad (6)$$

For all practical purposes, $2RT/E << I$ and hence can be neglected. Thus the Eq. (6) reduces to the following

$$\ln\left[\frac{g(\alpha)}{T^2}\right] = \ln\left(\frac{AR}{\beta E}\right) - E/RT \quad (7)$$

where α is the fractional loss of the sample at temperature T and $g(\alpha)$ is a function of α and governs the type of mechanism that the reaction follows. A plot of $\ln[g(\alpha)/T^2]$ *vs.* $1/T$ should result in a straight line with a slope of $-E/R$ and intercept of $\ln(AR/\beta E)$. Thus the activation energy (E) and pre-exponential factor (A) can be determined from the slope and intercept, respectively.

The entropy of activation (ΔS^*) can be estimated using the following Eq. (8).

$$A = \left(\frac{KT_i}{h}\right)\exp\left(\frac{\Delta S^*}{R}\right) \quad (8)$$

which on rearranging gives

$$\Delta S^* = R\ln\left(\frac{Ah}{KT_i}\right) \quad (9)$$

where h – Planck's constant, k – Boltzmann's constant and T_i – decomposition's peak temperature from TG curve.

All probable forms of $g(\alpha)$ used for identification of the reaction mechanism [21] has been evaluated as per Jeyanthi [22], Jurka *et al*. [23] and Abd Alla *et al*. [24]. However unless a statistical approach is used, it is difficult to identify the most suitable reaction mechanism for a given thermal reaction. Equation (7) is of the form $Y=Ax+B$. Hence for a single TG curve, one can use all the $g(\alpha)$ functions [20] and the one which has the best linearity would be considered as the most probable mechanism. The correlation coefficient R^2, error in estimation of intercept and slope, S_b are used to test the linearity. The nearer R^2 approaches unity and the smaller error in estimation of intercept and slope, S_b the better is the linearity.

In the present investigation, a program has been developed using Macros to calculate these kinetic parameters from the non-isothermal TG curves. After feeding the values of a corresponding temperature and number of data points, the program calculates $\ln g(\alpha)/T^2$, $1/T$, slope, intercept, R^2 and error values for all the thirty reaction mechanisms [22] and prepares corresponding charts.

The kinetic parameters such as A, E and 'frequency factors' are calculated for all the synthesized products and the data are presented in Table 2.

TG data analysis

The data on temperature and percent mass loss have been subjected to differentiation to fix the actual number of stages involved in the process. Percentage mass loss was differentiated with respect to temperature and each time change in the sign of slope observed, it is presumed that there is a change in chemical reaction.

Model considered

The data has been analyzed to study the best fit model among the 30 models [22]. For fixing the best fit model, linear regression analysis has been carried out on all the models; the model that has R^2 closest to one has been chosen as the best fit model. When R^2 is identical for any of the two or more models, error in estimation of slope and constant were taken into consideration and the model that has least error in estimation of slope and constant, has been chosen to be the best fit.

Discussion

The thermal curve of the formaldehyde modified soy protein concentrate could be dissected into five steps (Figs 1–4). In case of sample SN6, the first break takes place around 237°C having mass loss about 5%, the second break takes place around 382°C having mass loss of about 48%, the third break takes place around 563°C having mass loss about 69% and the fourth break takes place around 710°C having mass loss of about 91%. This can be explained by considering the structure of soy-protein. It is well known [3] that the three dimensional structure of soy-protein is governed by its primary structure i.e. the sequence of amino acids. Two kinds of covalent bonds mainly found in proteins are: one is the peptide bond between the amino acid residues and the other is the disulfide bond. The other non-covalent bonds present in protein are electrostatic and hydrophobic interactions and the hydrogen bonding [25].

The first break around 237°C is attributed to the elimination of water and the dissociation of the quaternary structure of proteins. Further it is well known [3] that beyond 100°C the protein denatures their subunits and promotes the formation of protein aggregates via electrostatic, hydrophobic and disulfide interchange bonding mechanisms. This has been recently substantiated by Kilara and Sharkasi [26]. It is generally accepted that hydrophobic and disulfide bonding is involved and responsible for protein-protein aggregation

Table 2 The forms of $g(\alpha)$ used for kinetic parameters calculation

Function group	Mechanism	$g(\alpha)$
Accelerated α–t curve	Power law	
	P_4	α
	P_1	$\alpha^{1/4}$
	P_2	$\alpha^{1/3}$
	P_3	$\alpha^{1/2}$
	P_5	$\alpha^{2/3}$
S-shaped α–t curve	Exponential law	$-\ln\alpha$
	Avrami–Erofeev law	
	$A_{1.5}$	$[-\ln(1-\alpha)]^{2/3}$
	A_2	$[-\ln(1-\alpha)]^{1/2}$
	A_3	$[-\ln(1-\alpha)]^{1/3}$
	A_4	$[-\ln(1-\alpha)]^{1/4}$
	Prout–Tompkins law	
	B_1	$[-\ln(1-\alpha)]^{2}$
	B_2	$[-\ln(1-\alpha)]^{3}$
	B_3	$[-\ln(1-\alpha)]^{4}$
Phase boundary reaction in contracting area	R_1	$[1-(1-\alpha)^{1/2}]$
Phase boundary reaction in contracting volume	R_2	$[1-(1-\alpha)^{1/3}]$
1-Dimensional diffusion	D_1	α^2
2-Dimensional diffusion	D_2	$(1-\alpha)\ln(1-\alpha)+\alpha$
3-Dimensional diffusion; Jander equation	D_3	$[1-(1-\alpha)^{1/3}]^2$
3-Dimensional diffusion; Ginstling–Brounshtein equation	D_4	$[1-2/3\alpha]-(1-\alpha)^{2/3}$
Chemical reaction of first order	F_1	$-\ln(1-\alpha)$
Chemical reaction of second order	F_2	$1/(1-\alpha)$
Chemical reaction of third order	F_3	$1/(1-\alpha)^2$
	H_1	$[1-(1-\alpha)^{1/4}]$
	H_2	$(1-\alpha)^{1/2}$
	H_3	$[(1-\alpha)^{1/3}-1]^2$
	H_4	$[1-(1-\alpha)^{1/3}]^{1/2}$
	H_5	$[1-(1-\alpha)^{1/2}]^{1/2}$
	H_6	$1-(1-\alpha)^2$
	H_7	$1-(1-\alpha)^3$
	H_8	$1-(1-\alpha)^4$

caused by heating to temperature above 100°C. Further during this period the electrostatic and hydrogen bonding is also affected. The second break between 243 to 382°C is mainly due to the cleavage of the covalent bonding between the peptide bonds of amino acid residues. During this period 60% of phenyl-alanine and tryptophan residues and 80% of tyrosine residue are burnt. Further heating also causes three simultaneous reactions in the structure of soy protein. First, the dissociation of 7S and 11S protein subunits; second, the unfolding of the subunit secondary structure and third, the re-association of denatured subunits via disulfide, hydrophobic, electrostatic and other important bonding forces. The third break between 388 to 583°C is probably due to cleavage of S–S, O–N and O–O linkages of the protein molecule. The fourth break between 589–710°C is attributed to complete decomposition of protein molecule forming various gases like CO, CO_2, NH_3, H_2S and other gases. Beyond 710°C only the char residue remains.

It is observed in sample SN_6 that the initial step followed P1 mechanism while all other samples followed B1 (Prout Tompkins law) mechanism. It is also ob-

Table 3 Kinetic parameters of the cross-linked soy protein concentrate with formaldehyde

	Steps	Temperature range		Model	*R*-squared	Slope	Intercept	*E*/kJ mol^{-1}	Frequency factor
		Start	End						
SN6	1	73.12	236.75	P1	0.95871	–525.126	6.399	9.618	9.64E+02
SN6	2	242.74	381.71	B1	0.98324	–1767.995	8.506	32.382	2.67E+04
SN6	3	387.72	582.87	B1	0.97577	–1783.108	8.058	32.659	1.72E+04
SN6	4	588.86	709.65	B1	0.97152	–3836.597	10.032	70.270	2.66E+05
SN6	5	715.42	730.02	H3	0.99335	–16834.250	174.541	308.332	3.26E+78
SN9	1	70.30	236.85	B1	0.96343	–661.162	6.781	12.110	1.78E+03
SN9	2	242.85	393.62	B1	0.98060	–1741.770	8.441	31.902	2.46E+04
SN9	3	399.63	619.18	B1	0.97642	–1731.102	7.944	31.706	1.49E+04
SN9	4	625.06	734.31	B1	0.96621	–4285.984	10.397	78.501	4.29E+05
SN9	5	740.16	762.90	H3	0.98766	–13966.783	141.814	255.812	1.66E+64
SN10	1	68.60	238.41	B1	0.96158	–664.265	6.774	12.167	1.77E+03
SN10	2	244.40	383.08	B1	0.98181	–1808.592	8.562	33.126	2.89E+04
SN10	3	389.09	497.39	B1	0.98158	–2435.821	9.070	44.614	6.46E+04
SN10	4	503.47	552.09	B1	0.98353	–5365.119	12.452	98.266	4.19E+06
SN10	5	558.08	676.04	B1	0.96534	–3516.106	9.785	64.400	1.91E+05
SN10	6	681.93	707.97	H1	0.99594	–51727.449	58.614	947.427	4.51E+27
SN11	1	57.63	236.91	B1	0.96226	–684.875	6.862	12.544	2.00E+03
SN11	2	242.92	393.99	B1	0.98078	–1725.304	8.412	31.600	2.37E+04
SN11	3	399.99	593.42	B1	0.97490	–1824.270	8.087	33.413	1.81E+04
SN11	4	599.39	710.74	B1	0.96494	–3978.091	10.167	72.862	3.16E+05
SN11	5	716.62	747.85	H3	0.99471	–131216.515	13.618	240.333	5.57E+61

served the final step in sample SN_{10} followed H1 mechanism while other samples followed H3 mechanism.

A cursory glance at Table 3 regarding the values of activation energy for various steps of degradation is very interesting. The degradation as depicted in the thermal curve takes place in five steps. The values of the activation energy in case of all the four samples in the first step is very low indicating very fast degradation process. Subsequently the activation energy increases from the second step through the fourth step and becomes very high at the fifth step of the degradation indicating that this degradation becomes slower and slower and in the last step it is the slowest. This mechanism of degradation of the cross-linked soy-protein concentrate agrees well with the predicted mechanism.

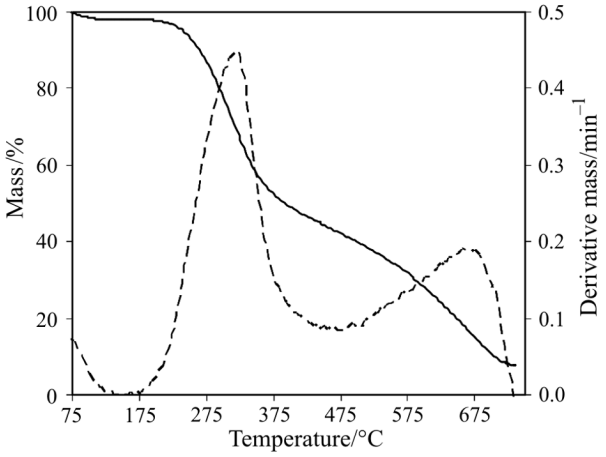

Fig. 1 TG curve and derivative curve for sample-SN6

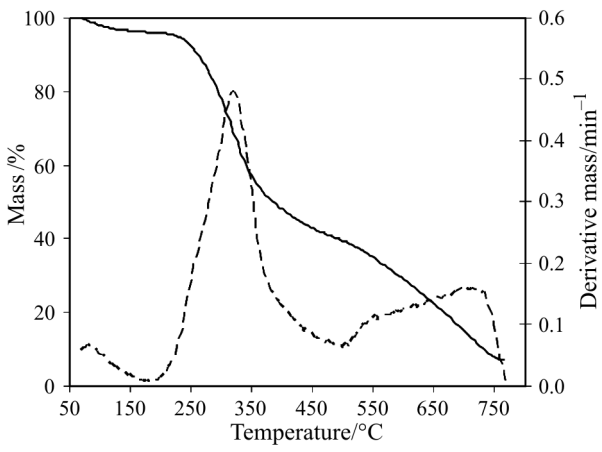

Fig. 2 TG curve and derivative curve for sample-SN9

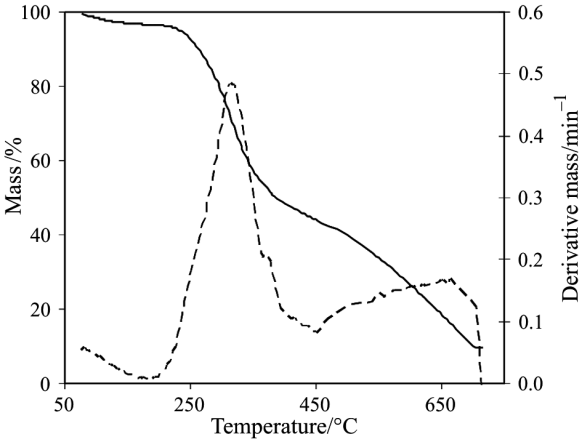

Fig. 3 TG curve and derivative curve for sample-SN10

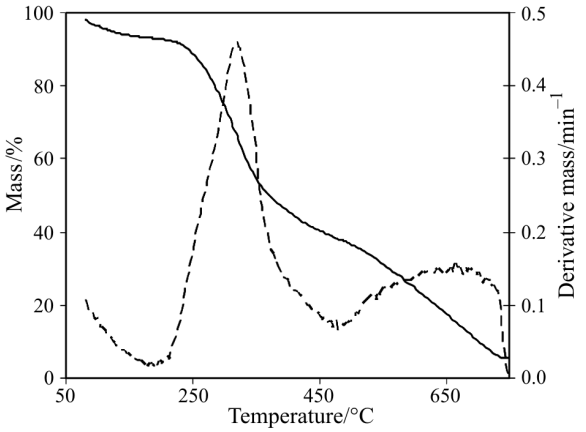

Fig. 4 TG curve and derivative curve for sample-SN11

Acknowledgements

The authors are grateful to CSIR, New Delhi for financial assistance [CSIR Project No. CSIR[21] 0496/01/EMR-11 dt.27.04.2001] and to Prof. R. K. Kar, Principal, Ravenshaw College, Cuttack, India for providing necessary facilities and encouragement.

References

1 X. S. Sun, H. R. Kim and X. Mo, JAOCS, 76 (1999) 117.
2 P. L. Nayak, J. Macromol. Sci. Rev. Macromol. Chem. Phys., C39 (1999) 481.
3 S. N. Swain, S. M. Biswal, P. K. Nanda and P. L. Nayak, J. Polym. Envir., l2 (2004) 35.
4 W. J. Wolf, J. Agric. Food Chem., 18 (1970) 967.
5 R. C. Roberts and D. R. Briggs, Cereal Chem., 42 (1965) 72.
6 K. Saio, I. Satoh and T. Watanabe, J. Food Sci., 39 (1973) 777.
7 K. Saio and W. Watanabe, J. Texture Stud., 9 (1978) 135.
8 J. B. German, T. E. O'Neil and J. E. Kinsella, J. Am. Oil Chem. Soc., 62 (1985) 1358.
9 T. Ya. Bogracheva, E. E. Braudo and V. B. Tolstoguzov, Food Hydrocolloids, 4 (1980) 1.
10 H. Zhang, M. Takenaka and S. Isobe, J. Therm. Anal. Cal., 75 (2004) 719.
11 R. Kumar, V. Choudhary, S. Mishra and I. K. Varma, J. Therm. Anal. Cal., 75 (2004) 727.
12 J. Bjorksten, Adv. Protein Chem., 6 (1951) 343.
13 S. Wang, H. J. Sue and J. L. Jane, Pure Appl. Chem., A33 (1996) 557.
14 S. Zhang, P. Mungara and J. Jane, Polym. Preprints, 39 (1998) 162.
15 J. Šesták, Talanta, 13 (1966) 567.
16 E. S. Freeman and B. Carrol, J. Phys., Chem., 62 (1958) 394.
17 C. D. Doyle, in 'Techniques and Methods of Polymer Evaluation', P. E. Slade and L. T. Jenkins (Eds), Chap. 4, Marcel-Dekker, New York 1966.
18 A. W. Coats and J. P. Redfern, Nature, 201 (1964) 68.
19 H. H. Horowitz and G. Metzger, Anal. Chem., 35 (1963) 1464.
20 J. Chacho and G. Parameswaran, J. Thermal Anal., 29 (1984) 3.
21 X. Gao and D. Dollimore, Thermochim. Acta, 215 (1993) 47.
22 S. Jeyanthi, Thermal studies on strontium oxalate doped with lanthanides, Ph. D. Thesis, Utkal University India 2004, p. 157.
23 B. Jurka, I. Salageanu and E. Segal, J. Therm. Anal. Cal., 62 (2000) 845.
24 E. M. Abd Alla and M. I. Abdel-Hamid, J. Therm. Anal. Cal., 62 (2000) 769.
25 C. V. Morr, JAOCS, 67 (1990) 265.
26 A. Kilara and T. Y. Sharkasi, Crit. Rev. Food Sci. Nutr., 23 (1986) 323.

Received: November 14, 2003
In revised form: June 30, 2004